

Polyaniline-Poly (*o*-methoxyaniline) composite films as supports of Pt-Ru nanoparticles for formic acid electro-oxidation

Qizhi Dong, Liying Zhu, Hansheng Wan, Cancheng Guo^{}, Gang Yu*

State Key Laboratory of Chemo/Biosensing and Chemometrics, College of Chemistry and Chemical Engineering, Hunan University, Changsha 410082, China

*E-mail: ccguohnu@163.com

Received: 24 August 2014 / Accepted: 9 October 2014 / Published: 28 October 2014

Polyaniline-Poly (*o*-methoxyaniline) (PANI-POMAN) composites are synthesized using cyclic voltammetry (CV) methods. Platinum (Pt) and Ruthenium (Ru) bimetal nanoparticles are co-deposited onto the PANI-POMAN film to produce a durable and efficient electro-active catalyst for formic acid oxidation. The morphology of composite/catalysts is characterized by scanning electron microscopy (SEM) and transmission electron microscopy (TEM). The electrocatalytic activity of the catalysts toward formic acid oxidation is investigated using CV and other electrochemical methods. The metal nanoclusters having average particle size of 5 nm as measured directly from TEM images. The PANI-POMAN supported bimetallic catalyst exhibits two times higher catalytic activity than that for pure PANI supported catalyst, and has a much better stability. The high activity is due to the unique porous and layered structure, high surface area, and uniform distribution of Pt-Ru nanoparticles. The enhanced stability is attributed to the introduction of Ru metal into Pt catalyst to display a synergistic effect, and the ability to reduce the propensity of poisoning of the catalyst by the intermediate products.

Keywords: Polyaniline; poly (*o*-methoxyaniline); bimetallic catalyst; Pt-Ru nanoparticles; formic acid; electrocatalytic oxidation

1. INTRODUCTION

Proton exchange membrane fuel cells (PEMFCs) are still limited by the challenges in hydrogen storage and transportation. In direct methanol fuel cells (DMFCs), methanol is flammable and poisonous. The intermediates generated during methanol oxidation can poison the catalysts and reduce the activity. Recently, it is these limitations of hydrogen and methanol that have increased interest in direct formic acid fuel cells (DFAFCs) [1-29]. Fuel cells using formic acid as the fuel has received much attention because such devices could overcome the limitations of both PEMFCs and DMFCs.

DFAFCs use structures and mechanisms similar to DMFCs, but have several advantages [30]. Formic acid is easy to oxidize, non-flammable, safe and environmentally friendly, and has low permeability. However, DFAFCs are limited by poor long term stability, and the Pd catalyst can be easily oxidized [31,32]. Therefore, developing durable highly efficient catalysts for anode is of a great interest for this application.

Pure Pt electrode is easily poisoned by the intermediates such as COads in the formic acid oxidation process, thus reducing the electrocatalytic activity of electrode. In order to improve the electrocatalytic activity of Pt electrode, significant effort has been devoted to develop different types of Pt catalysts and Pt alloy catalysts by various synthetic methods [33-35]. As a synergic effect of alloying, Pt-Ru showed a much higher activity than pure Pt due to the rapid dehydrogenation reaction on Pt and the enhancement in CO₂ production rate by the effective removal of COads formed in the dehydration reaction, which is referred to a bifunctional mechanism analogous to methanol oxidation. In addition to Pt-Ru bimetal, platinum surfaces have been modified by electrodeposition, not involving the formation of alloy, with various elements such as Pd, Pb, As, and Bi attempts to avoid poisoning and the resulting products show an increase in apparent reaction rate for formic acid oxidation [36].

To improve dispersion and utilization of metal catalysts, they were usually supported by a high-area material. The most widely used catalyst support is amorphous carbon powders currently. In order to search the optimum catalyst support, various special sizes and morphologies of materials have been extensively studied [37, 38]. Polyaniline (PANI), as one of electrically conducting polymers, has been intensively investigated. PANI is one of the most promising catalyst supports because of its high electrical conductivity, relatively friendly environment, highly accessible surface area, high chemical stability, and comparatively low cost. It has been reported that PANI film can significantly improve the dispersion of the supported metal particles and the ability for CO antipoisoning due to the acceleration of oxygen-donating species formation [39, 40]. In addition, PANI also has good proton transfer capability in an acidic medium. It is especially beneficial for reactions in proton exchange membrane fuel cells (PEMFCs), where proton ions are produced at the anode and consumed at the cathode.

Currently Pt catalysts supported on conductive polymers such as polyaniline and its derivatives are investigated. PANI and its derivatives have been considered promising materials for batteries and the catalysis of electrochemical reactions [41]. The presence of PANI in the catalyst layer increases catalyst utilization [42] and reduces the polarization resistance of the DFAFCs due to the electronic conductivity of PANI and the proton conductivity afforded by monomers retained in the PANI network [43]. However, Polyaniline (PANI) usually has a fibrous morphology with larger interconnected pores. Although the metal particles deposited on this substrate is in tens nanometer size, but the particles are normally deposited inside the pores rather than on the surface. Poly (*o*-methoxyaniline) (POMAN), has been extensively investigated due to its solubility in different media, good electrochemical properties, high solubility and thermodynamic stability [44]. However, pure POMAN has problems including small specific surface area and large metal particles deposited inside the pores rather than on the surface. Another factor that also influences the electroactivity of the electrode is the method used for the electrodeposition of metallic particles [36, 44]. Particles size and their distribution are important parameters since they relate to the real surface area [43].

In this work, a simple approach is demonstrated to overcome these limitations using PANI-POMAN composites and bimetallic catalysts. The PANI-POMAN composites are synthesized through CV method with a large platinum mesh as counter electrode. Pt and Ru metals are co-deposited onto the PANI-POMAN films to prepare a Pt-Ru/PANI-POMAN composite as the catalyst and its electrocatalytic activity and morphology are investigated by SEM, TEM and electrochemical methods. The electrocatalytic performance of PANI-POMAN supported Pt and Pt-Ru bimetal catalyst to formic acid oxidation are systematically studied. The results show that the dual-polymer system has much higher electrocatalytic activity compared with a single polymer system. In addition, the introduction of Ru metal can reduce intermediate formation such as COads during oxidation process, significantly enhancing the Pt activity in the direct oxidation reaction, and further improving the oxidation activity of the binary metal catalyst.

2. EXPERIMENTAL SECTION

2.1 Chemicals and Instruments

Chloroplatinic acid (H_2PtCl_6), ruthenium chloride hydrate ($\text{RuCl}_3 \cdot n\text{H}_2\text{O}$), formic acid (HCOOH), *o*-methoxyaniline, and aniline were purchased from Sinopharm Chemical Reagent Co (China). All chemicals used in this paper were of analytical grade. Water used here was double distilled water. Reference electrochemical workstation was from Gamry Co (3000, USA). A platinum electrode (working area being 0.71 cm^2) was used as the working electrode. A large platinum mesh was used as the counter electrode, and a saturated calomel electrode (SCE) as the reference electrode. Scanning electron microscopy (SEM, S-4800, Hitachi, Japan) equipped with an energy-dispersive X-ray analyzer (EDX, S-4800, Hitachi, Japan) and transmission electron microscopy (TEM, JEOL, Japan) were used to characterize the morphology and structure of the samples. Crystallinity was evaluated by X-ray diffraction (XRD) (Rigaku D/max 2500) performed on a Bruker d8 diffractometer system equipped with a $\text{Cu K}\alpha$ radiation and a graphite monochromator operated at 40 kV and 250 mA.

2.2 Catalyst Preparation

Before experiments, the working electrode was pretreated by polishing, washing, and drying at room temperature. Then the pretreated platinum working electrode was placed into a three electrode reaction bath containing $0.3 \text{ mol}\cdot\text{dm}^{-3}$ monomer and $0.5 \text{ mol}\cdot\text{dm}^{-3}$ sulfuric acid. The PANI and POMAN films were synthesized by CV methods using the optimum conditions (such as potential, scan rate) identified by this study. The mass of the polymer films (W_{polymer}) was calculated from the total charge passed through the cell during the film growth process, according to Eq. (1) [45]:

$$W_{\text{polymer}} = \frac{(\eta Q_{\text{dep1}})(M_1)}{F(Z_1)} \quad (1)$$

Here, W_{polymer} is calculated by using the charge (Q_{dep1}), assuming a 100% current efficiency (η) (the total charge passed through the cell during the polymer film growth process); M_1 is the molecular

weight of polyaniline and its derivatives; F is the Faraday constant (96485 C/mol); and Z_1 is the number of electrons transferred per monomer attached to the polymer, in which $Z_1=2+\delta$ [46–47]. The partial charge δ is called the doping level. The calculated δ is about 0.25 for different precursors in the experiments, assuming a 100% current efficiency (η), according to Eq. (2) [48]:

$$\delta = \frac{2Q_0}{\eta Q_d - Q_0} \quad (2)$$

Where Q_d is the total charge used for polymer deposition and Q_0 is the total charge of oxidized species in the polymer films. The different types of polymer films prepared by above mentioned method were placed into a 0.5 mol·dm⁻³ sulfuric acid solution containing different concentration ratios of H₂PtCl₆ and RuCl₃ for 15 minutes, allowing the metal ions to penetrate the polymer layer and be deposited on the film uniformly. The scanning voltage for catalyst deposition was -0.25 to 0.65V with a scanning rate of 10 mV·s⁻¹. The CV scan was repeated 15 times (total 540s). After modification, the electrodes were washed in deionized water and dried at room temperature, then cycled in 0.5 mol·dm⁻³ H₂SO₄, between -0.2 V and 0.65 V vs. SCE at a scan rate of 10 mV·s⁻¹ in order to remove surfactant residues from the surface and measure its electrochemical area. The amount of Pt (W_{Pt}) loaded onto electrode was determined by the following Eq. (3) [45, 49]:

$$W_{Pt} = \frac{(\eta Q_{dep2})M}{FZ} \quad (3)$$

Where Q_{dep2} is the integrated charge during platinum deposition assuming a 100% current efficiency, M is the atomic weight of Pt, Z is the number of electrons transferred (taken as 4 for the formation of Pt), and F is the Faraday constant. In this paper, the amount of Pt deposited are 0.26 mg and the mass of the polymer films in all the cases and 3.26 μg, respectively. Formic acid electro-oxidation experiments were performed in a 1 mol·dm⁻³ HCOOH+0.5 mol·dm⁻³ sulfuric acid solutions purged with nitrogen. The electrocatalytic activity of the Pt-Ru modified composite electrodes were studied in 1 mol·dm⁻³ formic acid + 0.5 mol·dm⁻³ sulfuric acid mixture solution using CV methods (0 to 1.0 V potential range, 10 mV·s⁻¹ scan rate).

The integrated area under the adsorption peak in the CV curves represents the total charge concerning H⁺ adsorption, Q_H , and has been used to determine EASA by employing the equation(4)[50,51] :

$$EASA = \frac{Q_H}{0.21W_{Pt}} \quad (4)$$

The EASA of Pt is determined to be 211.36 m²·g⁻¹ for PANI-POMAN(1:1)/Pt-Ru(2:1), which is much larger than that of PANI-POMAN(1:0)/Pt-Ru(2:1) (69.982m²·g⁻¹), PANI-POMAN(0:1)/Pt-Ru(2:1)(116.60 m²·g⁻¹), PANI-POMAN(1:1)/Pt-Ru(1:1)(167.3 m²·g⁻¹), PANI-POMAN(1:1)/Pt-Ru(1:2) (107.6 m²·g⁻¹).

2.3 Electrochemical measurements

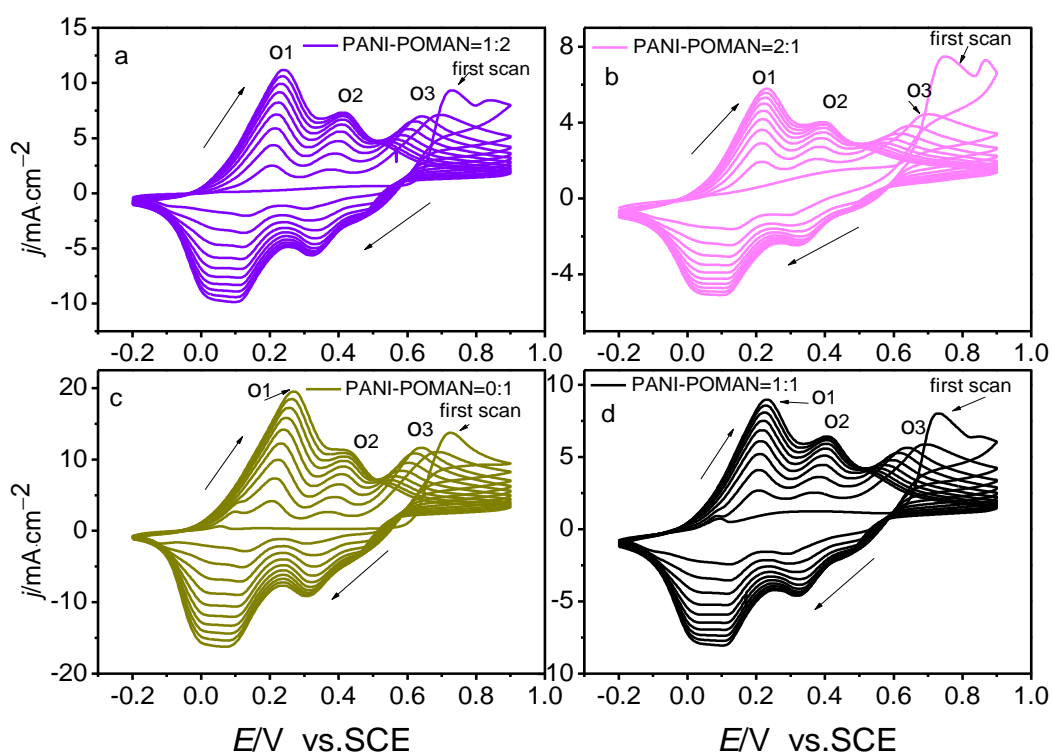
The electrochemical activity studies were performed by means of cyclic voltammetry (CV) and chronoamperometry methods on a Gamry Co (3000, USA) electrochemical workstation at room temperature in 0.5 mol·dm⁻³ H₂SO₄ or 0.5 mol·dm⁻³ H₂SO₄+1 mol·dm⁻³ HCOOH, after being purged

with N_2 for at least 10 min using a scan rate of $50 \text{ mV}\cdot\text{s}^{-1}$. A Pt mesh counter electrode was used as a SCE reference electrode. Electrochemical impedance spectroscopy (EIS) of the catalysts were carried out in $1 \text{ mol}\cdot\text{dm}^{-3} \text{ HCOOH} + 0.5 \text{ mol}\cdot\text{dm}^{-3} \text{ H}_2\text{SO}_4$ as supporting electrolyte. Impedance spectra of the polymers were taken moving from 100 k HZ to 10 m HZ at 5 mV vs.SCE.

3. RESULTS AND DISCUSSION

3.1 Electrochemical Synthesis of polymer films

The CV curves of the composite films in a $0.5 \text{ mol}\cdot\text{dm}^{-3}$ sulfuric acid solution + $0.3 \text{ mol}\cdot\text{dm}^{-3}$ different monomers (a, b, c, d) between -0.2 to $+0.9 \text{ V}$ scanning potential using a $10 \text{ mV}\cdot\text{s}^{-1}$ scanning rate (Fig.1). Three reversible oxidation peaks noted O1, O2 and O3 are observed, corresponding to PANI oxidation, oxidation from non-emeraldine oxidation state to emeraldine oxidation state and its further oxidation. The CV curves show that the potential of the three oxidation peaks increase positively with cycling, while the potential of the O3 reduction peak decreases with cycling. The peak current increases with the cycling during polymerization of aniline because PANI has good catalytic activity to aniline, promoting polymer deposition on the surface which was recognized as an “autocatalytic” behavior of PANI [43]. From Fig.1c, only one oxidation peak appears at 0.7 V when scanned positively starting -0.2 V , suggesting that *o*-methoxyaniline radical cations are formed on the surface of the platinum electrode, initiating the polymerization reaction. Three pairs of redox peaks appear from the second cycle. The first redox peak appears at 0.22 V , corresponding to the partial oxidation of completely reduced *o*-methoxyaniline.



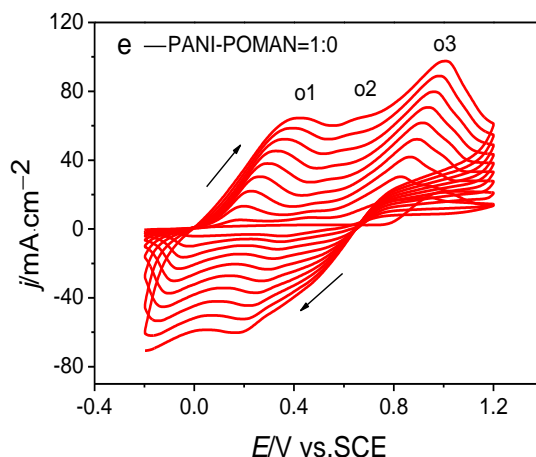


Figure 1. CVs of $0.15 \text{ mol} \cdot \text{dm}^{-3}$ monomer in a $0.5 \text{ mol} \cdot \text{dm}^{-3} \text{ H}_2\text{SO}_4$: a. PANI-POMAN (1:1), b. PANI-POMAN (1:2), c. PANI-POMAN (0:1), d. PANI-POMAN (2:1), e. PANI-POMAN (1:0)

The third pair of redox peak appears at 0.6 V, corresponding to the completely oxidation state of polymers. The peak current increases with cycling because *o*-methoxyaniline polymerization begins at the electrode surface and the self-catalytic reaction also starts at the same time. From the CV curves, three pairs of redox peaks increase uniformly, indicating that POMAN film is deposited continuously at the Pt electrode surface with a uniform structure. Fig.1d shows the continuous CV curves of Pt disk electrode in $0.5 \text{ mol} \cdot \text{dm}^{-3}$ sulfuric acid solution containing $0.15 \text{ mol} \cdot \text{dm}^{-3}$ aniline and *o*-methoxyaniline mixture solution.

As illustrated in CV curves, the polymer on the electrode surface also grows continuously and the current density of redox peaks increase with cycling, indicating the amount of polymer on the electrode increases gradually [52]. The monomer begins to be oxidized during the first positive scan at 0.6V with further polymerization as scanning continues. On the other hand, the resulting polymers are reduced at the first negative scanning. The electrochemical properties of Fig.1a and Fig.1b are similar to the PANI-POMAN (1:1), with three redox reaction steps. The first step(O1) is due to the conversion of fully reduced PANI-POMAN to imine, the second step(O2) is due to the oxidation of the groups on the two polymer terminals, the third step(O3) is due to further oxidation of imine to amine.

3.2. Morphological analysis of the films

In order to have good electrocatalytic properties, the polymer substrate itself should have good conductivity for fast charge transport, as well as stable porous structure to uniformly disperse Pt-Ru metal particles. Formic acid oxidation activity of the electrode is sensitive to the morphology of the composite film. Fig.2 shows the SEM images of the different electrode surfaces.

Fig.2.B.a, 2.B.b, 2.B.c and 2.B.d illustrate the electrodeposited metal particles morphology of the composite films. The metal nanoclusters are approximately sphere with an average diameter about 50 nm, some particles even as small as 10 nm (Fig.2.B.b and 2.B.d). Fig.2.B.a and 2.B.c show that two composite films have similar morphology with uniform metal particle distribution and less

agglomerates, which improves the utilization of the precious metals. However PANI-POMAN (1:1) films with different ratios of Pt to Ru (1:0 and 2:1) are different. From Fig.2.B.b and 2.B.d, Pt-Ru bimetallic particles not only have better dispersion than that of pure Pt particles, but also a rougher surface, suggesting a large surface area and good contact area to react with formic acid, for a higher electrocatalytic activity.

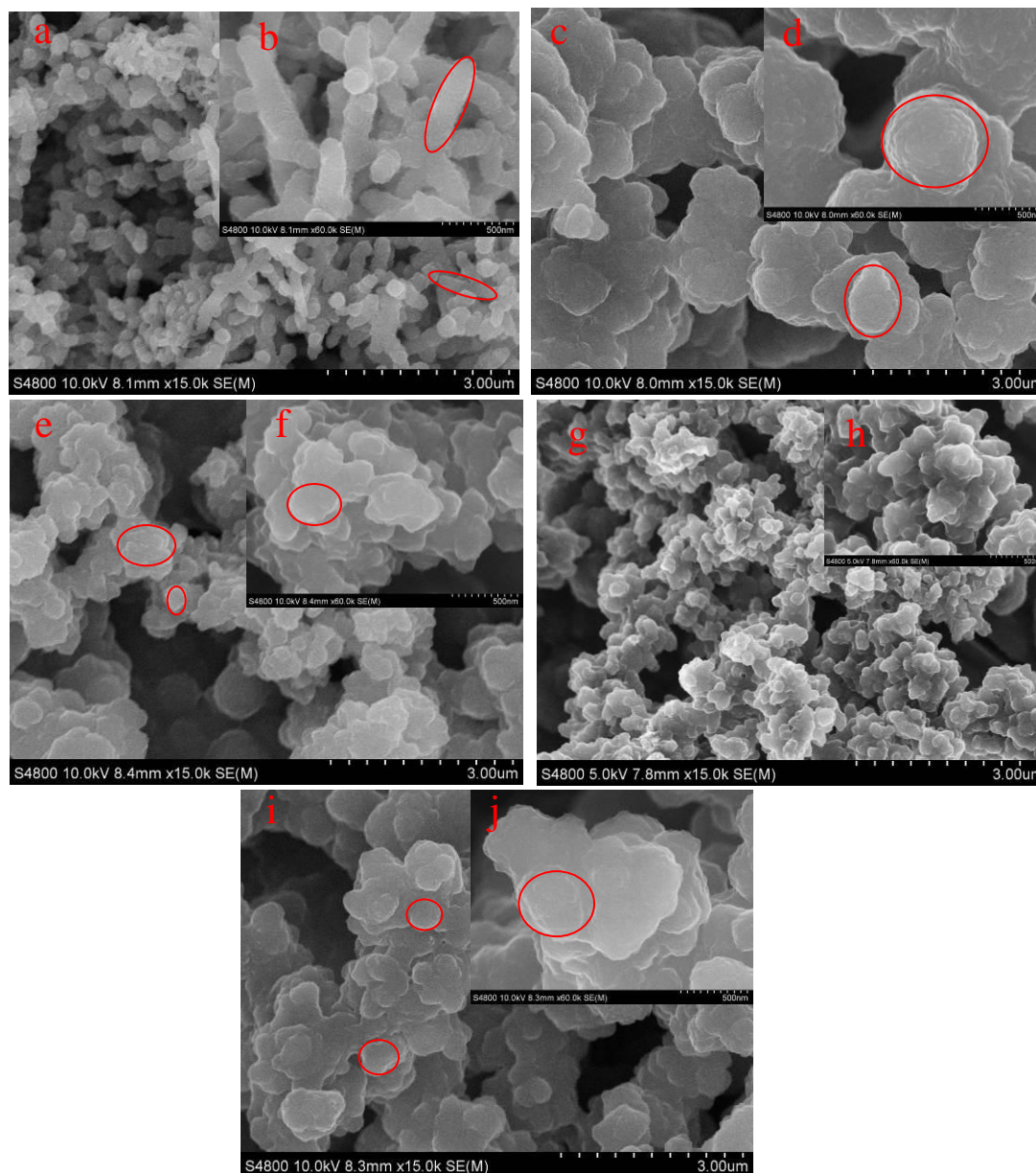


Figure 2.A SEM images of (a)(b) PANI-POMAN(1:0), (c)(d) PANI-POMAN(0:1), (e)(f) PANI-POMAN(2:1), (g)(h) PANI-POMAN(1:1), (i)(j) PANI-POMAN(1:2) film

The presence of 3D-cubic-like domains can facilitate molecular mass transport because it would allow that an interconnection exists between the pores, which are mainly parallel, nevertheless this would not be an important effect in our catalysts [53]. From Fig.2.A.a and 2.A.b, PANI has

nanofiber morphology with an average size of 10nm and Pt-Ru metal particles disperse uniformly on the substrate with the diameter of tens nanometers as in Fig.2.B.a. However, the Pt-Ru metal loading is low because of the weak interaction between the polymer substrate and the metal particles. As shown in Fig.2.A.c and 2.A.d, the morphology of the pure POMAN polymer substrate is cauliflower-like, with an average size of 60 nm and the bimetallic particles do not deposit exclusively on the polymer surface but are mainly located in the internal region [53], most metal particles are agglomerated. From Fig.2.A.e, 2.A.f, the morphology of PANI-POMAN (2:1) polymer is cauliflower-like with a small size of 50 nm, but the catalyst particles are large. From Fig.2.A.i, 2.A.j and Fig.2.B.k, 2.B.l, PANI-POMAN(1:2) film has a small size of 30 nm, although the size of metal particles deposited are small, but the metal particles are not well dispersed, resulting poor catalytic activity. From Fig.2.A.i, 2.A.j, the morphology of PANI-POMAN (1:1) polymer is plate-like with a small size of 20 nm and a large surface area, highly porous structure. The morphology of the Pt-Ru binary metal particles is sphere and the particles are uniformly dispersed on the three-dimension porous layered structure of the polymer substrate, achieving a highly dispersed bimetallic composite electrode catalyst.

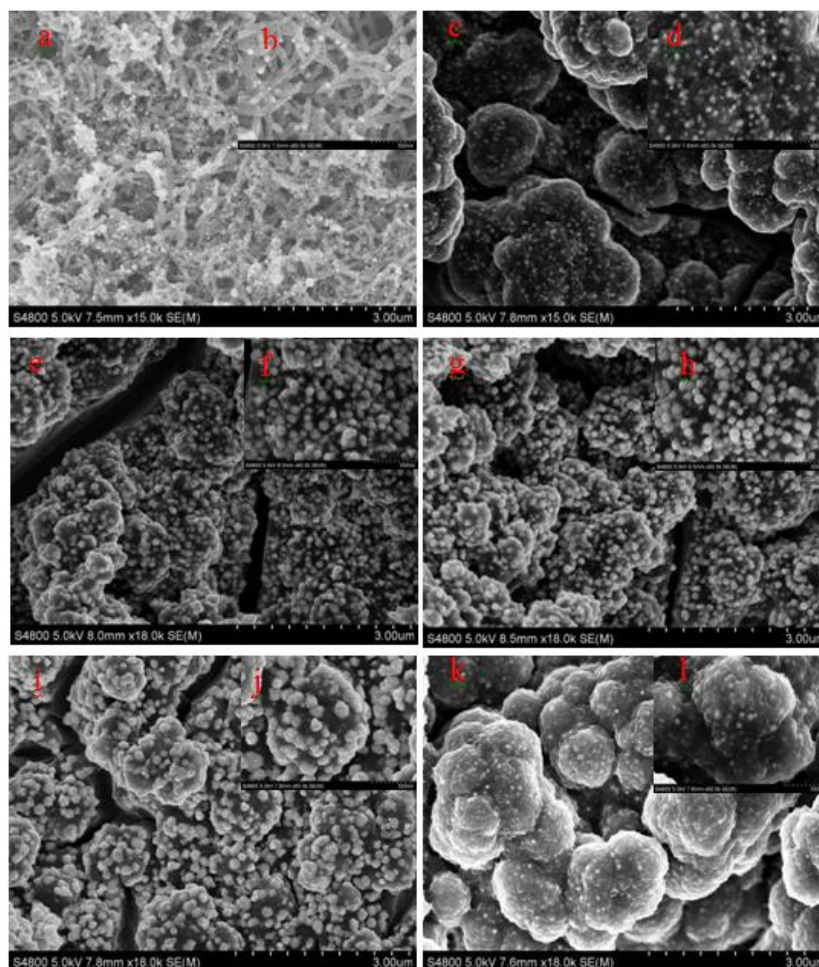


Figure 2. B SEM images of Pt-Ru(x:y)-PANI-POMAN(x:y) composite film electrode (a)(b).Pt-Ru(2:1)+PANI,(c)(d).Pt-Ru(2:1)+POMAN,(e)(f).Pt-Ru(1:0)+PANI-POMAN(1:1),(g)(h).Pt-Ru(2:1)+PANI-POMAN(1:1),(i)(j).PANI-POMAN(2:1)+Pt-Ru(2:1),(k)(l).Pt-Ru(2:1)+PANI-POMAN(1:2)

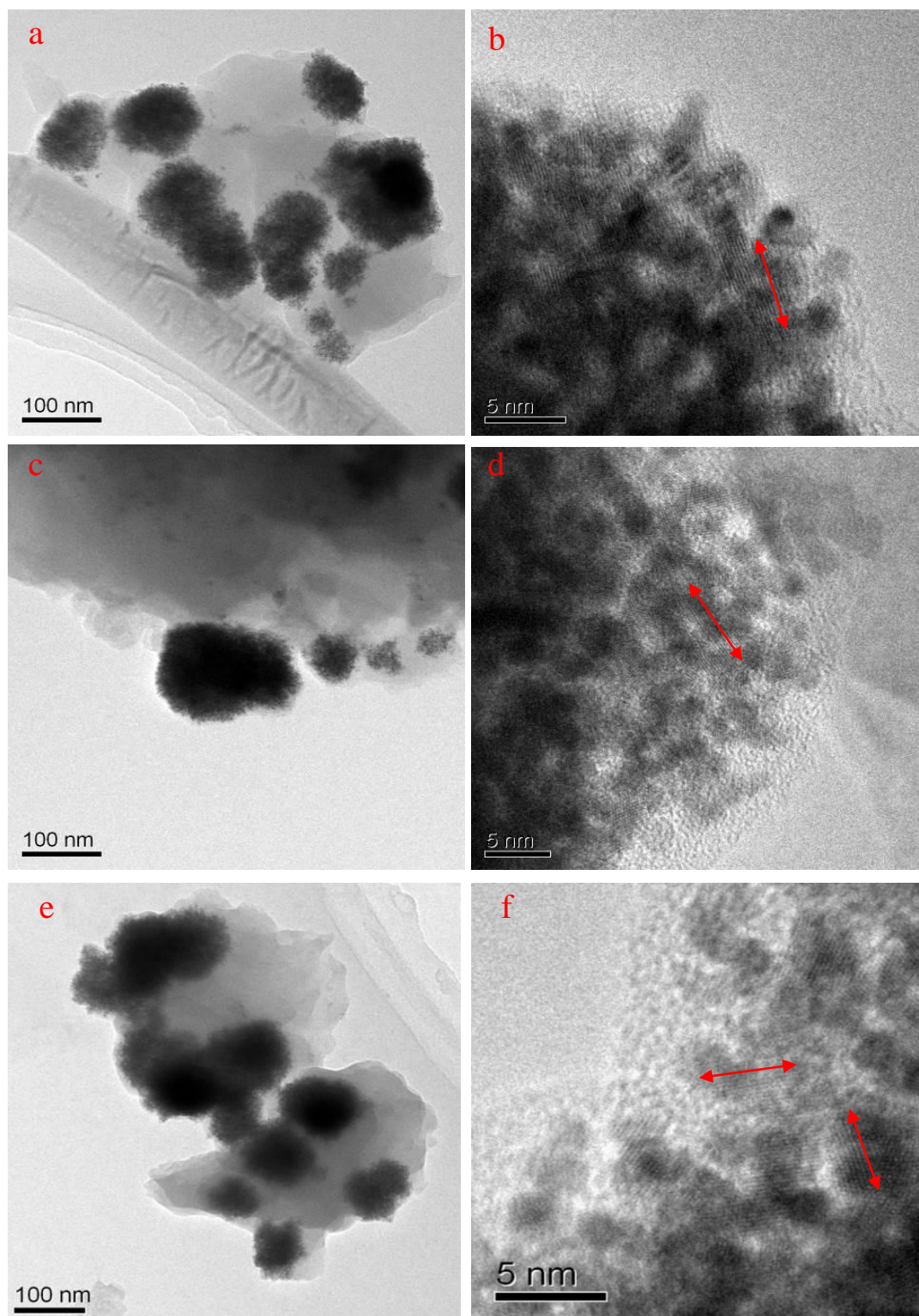


Figure 3. TEM images of different ratios of Pt-Ru bimetallic particles on PANI-POMAN (1:1) composite film: (a)(b). Pt-Ru(1:1)-PANI-POMAN(1:1), (c)(d). Pt-Ru(1:2)-PANI-POMAN(1:1), (e)(f). Pt-Ru(2:1)-PANI-POMAN(1:1) The double arrow represents crystal axis.

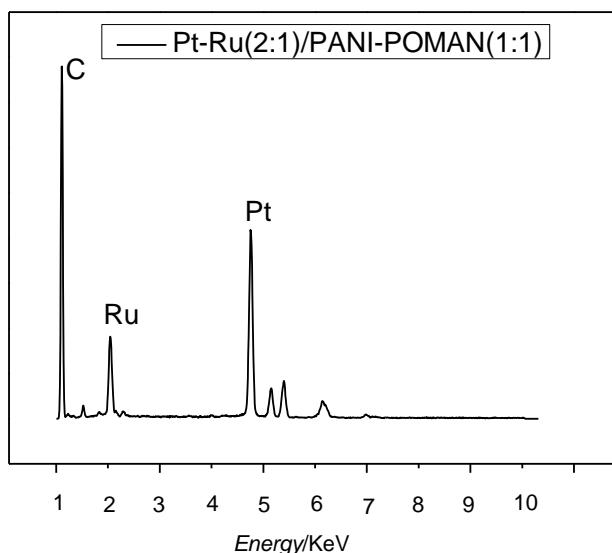


Figure 4. EDS spectrum of Pt-Ru(2:1)-PANI-POMAN(1:1) catalyst.

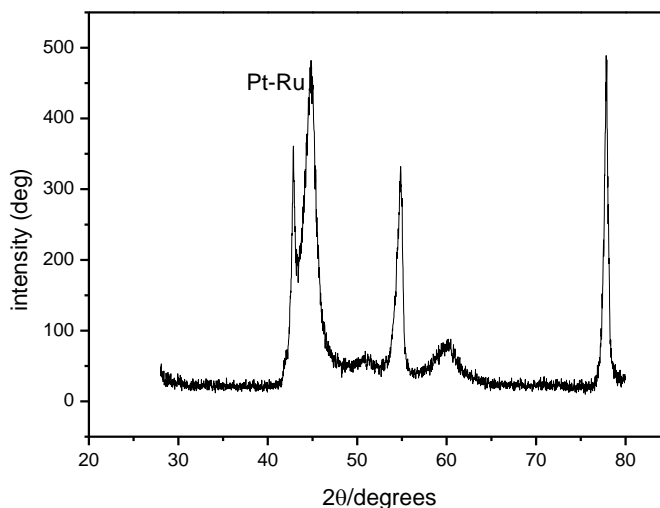


Figure 5. XRD patterns of Pt-Ru (2:1)-PANI-POMAN (1:1) catalyst

The TEM images (Fig.3) show that Pt and Ru particles have similar particle size and morphology. The average particle size is about 2 nm and the agglomerates are about 100 nm. Both Pt and Ru metals are detected in the energy dispersive spectroscopy (EDS) spectrum (Fig.4) and XRD (Fig.5). XRD analysis of the nanocomposite as-prepared and stored under ambient conditions reveals the presence of small amounts of Ru metal. From the high magnification images in Fig.3b and 3d, the metal particles are partially agglomerated because Ru nanoparticles are deposited at a lower potential occupying polymer substrate surface first. The higher the concentration of Ru metal in solution, the heavier the loading of Ru metal particles on the polymer substrate, the Pt particles can only accumulate deposition [54]. Comparing the three different microstructures with different Pt-Ru ratios, Pt-Ru (2:1) composite, with a rougher surface, irregular sphere, also has the best dispersion and least aggregation.

4. ELECTROCATALYTIC OXIDATION OF FORMIC ACID

The electrocatalytic oxidation of formic acid on Pt catalyst may have two pathways. The preferred pathway is a direct reaction, also called dehydrogenation reaction, in which formic acid is directly oxidized to CO₂ at low potentials (Equation 1). Another pathway is indirect reaction called dehydration reaction, in which formic acid is dehydrated to first form the intermediate product CO_{ads} and then oxidized at high potential to carbon dioxide[2,55,56](Equation 2). After introduction of Ru to Pt catalyst, the binary metal catalyst can reduce the intermediate such as CO_{ads} (Equation 3 and 4) and greatly improve the catalytic effect of Pt catalyst [57]:



Based on the above mechanism, the best way to improve the catalytic activity and enhance the poisoning resistance is to increase the direct oxidation and reduce the indirect oxidation of formic acid.

4.1 Effect of PANI to POMAN Ratio

The electrocatalytic properties and structure are not only related to the catalyst itself, but also to the support materials. The structure of the substrate materials greatly affect the dispersion and structure of deposited metal particles. It has been reported that PANI can significantly improve the dispersion of the supported metal particles and the ability for CO_{ads} antipoisoning due to the acceleration of oxygen-donating species formation [39].

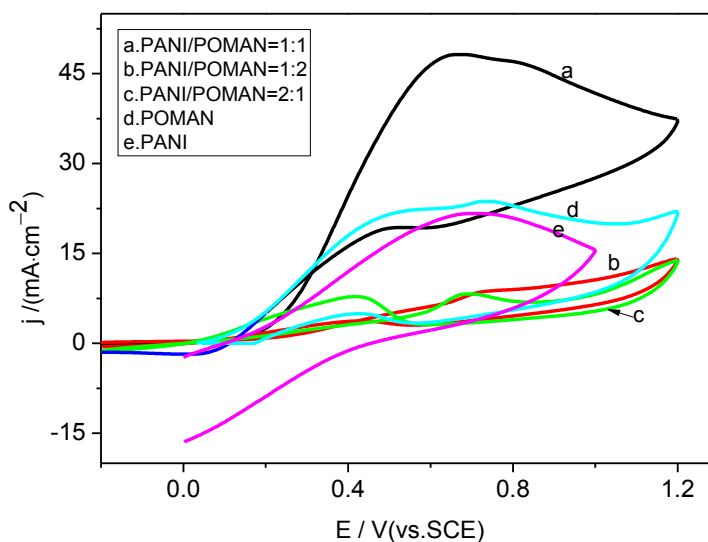


Figure 6. CV curves of Pt-Ru (2:1) modified composite film catalysts with different compositions of PANI to POMAN in a 1 mol·dm⁻³ HCOOH + 0.5 mol·dm⁻³ H₂SO₄ solution. The scanning potential is -0.2 to 1.2 V at 10 mV·s⁻¹

The conductivity of the substrate also affects the conductivity of the whole electrode, further affecting the catalytic activity. From early discussion, Pt-Ru (2:1) has the best dispersion and distribution on the PANI-POMAN substrate. By comparing the catalytic performance of Pt-Ru (2:1) modified PANI-POMAN film with different PANI to POMAN ratios, the optimal PANI-POMAN substrate can be obtained. Fig.6 shows the CV curves of Pt-Ru (2:1) modified catalysts with different PANI to POMAN compositions in a $0.5 \text{ mol}\cdot\text{dm}^{-3}$ sulfuric acid solution containing $1 \text{ mol}\cdot\text{dm}^{-3}$ formic acid. The scanning potential is -0.2 to 1.2V and the scanning rate is $10 \text{ mV}\cdot\text{s}^{-1}$.

As shown in Fig.6, for pure POMAN, PANI and PANI-POMAN (1:1), the current density begins to ascend at about 0.15 V during positive scan, and reaches a maximum of 1.3 , 22 and $47.5 \text{ mA}\cdot\text{cm}^{-2}$ at 0.66 V respectively. PANI-POMAN (1:1) composite has the highest current density at 0.66 V without any change in peak potential comparing with other composite film catalysts. The increase in the redox wave currents implies that the amount of polymer on the electrode ascends [58].

The introduction of *o*-methoxy group into the aromatic ring produces a steric repulsion between H and bulky the $-\text{OCH}_3$ group. It not only increases the crystallinity of polymers and the contact area with the metal particles [59], but also reduces the nanoparticle size. PANI-POMAN (1:1) composite modified by Pt-Ru (2:1) has the fastest electron transport. The metal particles can capture electrons from formic acid and oxidize formic acid easily.

4.2 Electrochemical impedance analysis

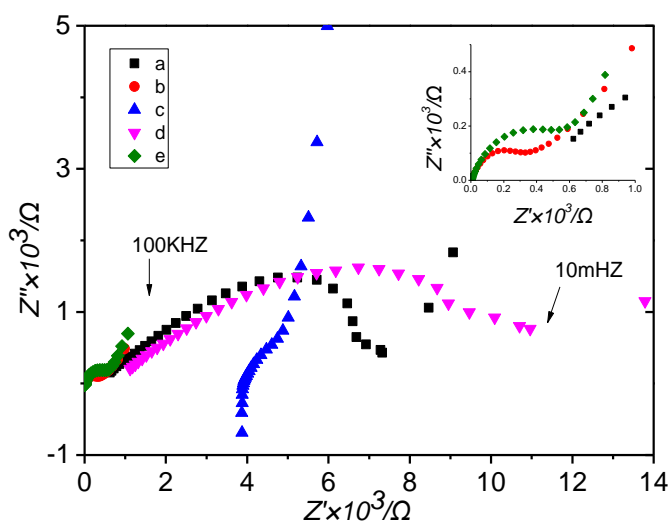


Figure 7. Electrochemical impedance spectroscopy (Nyquist plots) from 10 kHz to 10 mHz for electrodes a. Pt-Ru(2:1)-PANI, b. Pt-Ru(2:1)-PANI -POMAN (1:2), c. PANI-POMAN(2:1), d. Pt-Ru(2:1)-PANI-POMAN(2:1), e. Pt-Ru (2:1)-PANI-POMAN(1:1) at their open circuit potentials of 5mV (vs. SCE), respectively, in $1 \text{ mol}\cdot\text{dm}^{-3}$ HCOOH+ $0.5 \text{ mol}\cdot\text{dm}^{-3}$ H_2SO_4 , work area is 0.71 cm^2

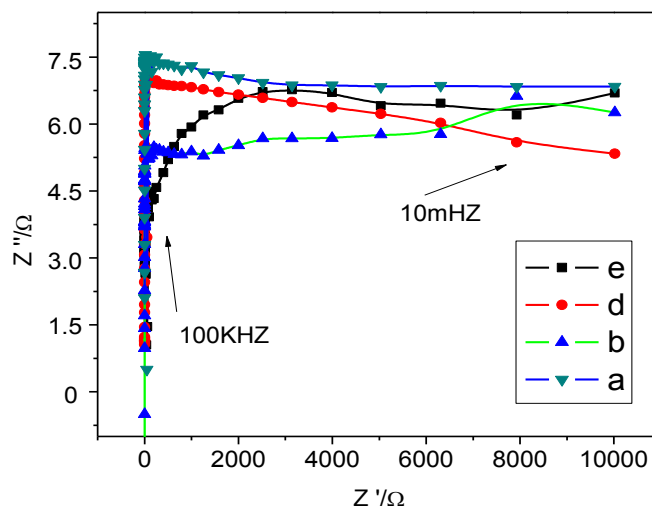


Figure 8. Electrochemical impedance spectroscopy (Nyquist plots) from 10 kHz to 10 mHz for electrodes a. Pt-Ru(2:1)-PANI, b. Pt-Ru(2:1)-PANI -POMAN (1:2), d. Pt-Ru(2:1)-PANI-POMAN(2:1), e. Pt-Ru (2:1)-PANI-POMAN(1:1) at their open circuit potentials of 5mV(vs. SCE), respectively, in $0.5 \text{ mol} \cdot \text{dm}^{-3} \text{ H}_2\text{SO}_4$, work area is 0.71 cm^2

Among electrochemical characterization techniques EIS represents a useful tool for the investigation of films because of the small perturbations involved in the operative conditions for the impedance measurements [59]. Fig.7 shows the electrochemical impedance results of five different composite films. All spectra have semblable shapes, with a semi-cycle in the high frequency region, and sloped line in the low frequency region [60].

The depressed semi-circle between the experimental points at 100.0 kHz and 100.0 MHz could be associated with the situation corresponding to an interface between a rough electrode and an electrolyte with occurrence of very slow faradaic process [61]. The diameter of the high frequency region is related to the electronic resistance of electrochemical reaction. The low frequency region is controlled by the diffusion process, and the cross-over point with the horizontal axis in the high frequency region is related to the resistivity of the electrolyte (R_{el}) [62]. The semi-cycle region suggests that the interfacial reaction between the polymer and the electrolyte is attributed to the double layer capacitance (C_{dl}) and the charge transfer resistance (R_{ct}). Pt-Ru (2:1) modified PANI-POMAN (1:1) (Fig.7e) has the smallest diameter in the high frequency semicircle region, indicating that this composite film has the lowest resistance due to the large surface area and good conductivity. Addition of POMAN to the polymer effectively increases the charge transfer between the electrolyte and the catalyst, resulting good electrocatalytic activity [57, 63-65].

However, the diameters of the 5 semicircles are greatly different. Comparing the four composite films in fig.7 (a), (b), (d) and (e), it indicated that the greater the concentration of polyaniline composite membrane impedance diagram, the larger the diameter of the semicircle in high frequency region, namely, the greater was the electrochemical reaction resistance. Therefore, poly-(*o*-methoxyaniline) possesses better solubility than polyaniline, for the reason that *o*-methoxy on the benzene ring structure in the presence of a methoxy group improves the crystallinity of the polymer [60], reducing the interface resistance of the polymer solution. Moreover, from the fig.8, the study of

which was undertaken under the condition of $0.5 \text{ mol} \cdot \text{dm}^{-3} \text{ H}_2\text{SO}_4$ solution in the absent of formic acid, it is shown that the impedance diagram, it is shown that the Pt-Ru (2:1) modified PANI-POMAN (1:1) in the high frequency region of maximum diameter of the semicircle represents the maximum catalyst solution resistance, owing to that the polymer film of poly-(*o*-methoxyaniline) content was less, the contact resistance of the composite film of the solution was greater.

4.3 Electrochemical catalytic effect of deposited Pt to Ru ratio

Ru metal as a bifunctional catalyst can provide oxygen containing species to oxidize intermediates for Pt in the formic acid oxidation process. The loading of Ru metal particles in the Pt-Ru bimetallic particles affect the further oxidation of the intermediate product [65, 66]. To study the effect of Pt-Ru concentration ratio to the electrocatalytic activity, the optimal PANI-POMAN (1:1) film is selected as catalyst substrate.

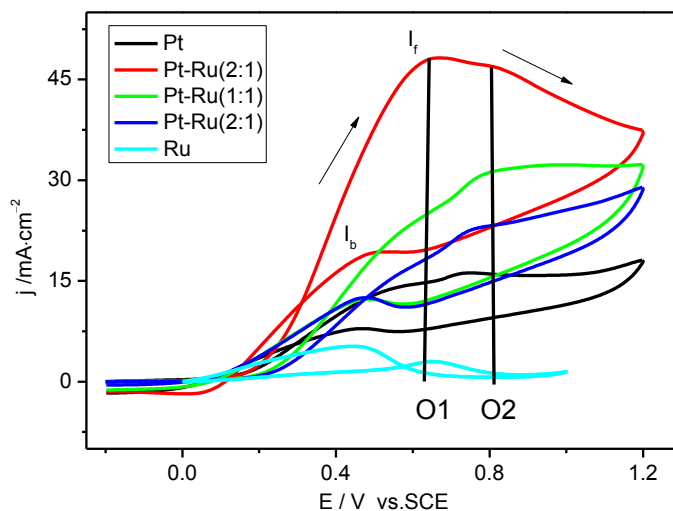


Figure 9. CV curves of composite electrodes with different deposition ratios of Pt to Ru in a $1 \text{ mol} \cdot \text{dm}^{-3} \text{ HCOOH} + 0.5 \text{ mol} \cdot \text{dm}^{-3} \text{ H}_2\text{SO}_4$ solution

Table 1. Catalytic properties of composite film with different concentration ratios of H_2PtCl_6 and RuCl_3 solutions

$(\text{H}_2\text{PtCl}_6:\text{RuCl}_3)/\text{mmol} \cdot \text{dm}^{-3}$	3:0	3:1.5	3:3	3:6
$j_{O1}/ \text{mA} \cdot \text{cm}^{-2}$	15.1	47.6	25.8	19.2
$j_{O2}/ \text{mA} \cdot \text{cm}^{-2}$	15.9	46.7	29.7	22.5
j_{O1}/j_{O2}	0.95	1.02	0.87	0.85
I_f/I_b	2.0	2.5	2.45	1.83
E_f/V	0.748	0.668	0.718	0.724

Into $3\text{ mol}\cdot\text{dm}^{-3}$ H_2PtCl_6 deposition solution, different concentrations of RuCl_3 are added to control the concentration ratio of Pt to Ru, thereby different compositions of Pt-Ru/PANI-POMAN(1:1) composite electrodes can be obtained. Table.1 lists all the oxidation results of the composite films.

Oxidation intermediates and oxygen containing species are produced on the electrode surface in the formic acid oxidation process during CV positive scanning; however, most of the intermediates and oxygen containing species are oxidized completely and the electrode surface is cleaned in the negative direction scanning [67]. From the CV curves of pure Pt and Pt-Ru (2:1) electrodes in the $0.5\text{ mol}\cdot\text{dm}^{-3}$ sulfuric acid solution containing $1\text{ mol}\cdot\text{dm}^{-3}$ formic acid (Fig.9), the first oxidation peak appears at about 0.67V, due to direct oxidation of formic acid; the second oxidation peak appears at 0.76V, due to indirect oxidation of formic acid, in which intermediates such as carbon monoxide are formed. A higher ratio of direct oxidation peak to indirect oxidation peak (j_{o1}/j_{o2}) suggests that the direct oxidation reaction is favored with less poisoning from carbon monoxide [68]. The first peak current density (j_{o1}) of Pt-Ru (2:1) electrode to formic acid oxidation is $47.6\text{ mA}\cdot\text{cm}^{-2}$ which is 3.2 times larger than that of pure Pt electrode ($15.1\text{ mA}\cdot\text{cm}^{-2}$). The ratio of oxidation current peak density at positive scanning I_f and I_b at negative scanning is an important index measuring the catalyst poisoning resistance. The larger the value of I_f/I_b , the stronger ability for the catalyst to remove the surface intermediates. The I_f/I_b value of Pt-Ru (2:1) electrode is 2.5 larger than that of pure Pt electrode (2.0), suggesting Pt-Ru (2:1) electrode has better electrocatalytic ability to formic acid oxidation than that of pure Pt electrode. As illustrated in Fig.9. , the oxidation of pure Pt electrode to formic acid is mainly through the indirect pathway, in which intermediates such as COads are produced on the electrode surface and reduce the electrocatalytic activity. On the other hand, Pt-Ru (2:1) electrode shows that the direct oxidation pathway is favored, in which less intermediates is produced. Thus, it is observed that a small amount of Ru in the composition of the catalyst enhances its catalytic activity [54]. These results suggest that adding Ru into Pt catalyst greatly improves the electrocatalytic performance toward formic acid oxidation. Ru metal atoms modify Pt surface and enhance the interaction between Pt and formic acid. Comparing the data from Table.1, Pt-Ru(2:1) modified PANI-POMAN(1:1) composite catalyst has the best electrocatalytic property toward formic acid oxidation, as well as the lowest peak voltage E_f at positive scanning which is shift 80 mV negatively comparing with pure Pt catalyst, suggesting formic acid is much easier to oxidize on the Pt-Ru(2:1)/PANI-POMAN(1:1) composite electrode.

Pt-Ru bimetallic catalysts have synergistic effect. At low potential H_2O molecules can be absorbed on the electrode surface and be decomposed by Ru metal to form RuOH, providing oxygen containing species for Pt to oxidize the carbon monoxide, therefore reducing the oxidation potential of catalyst and enhancing the poisoning resistance at the same time. The peak potential shifts negatively because RuOH is formed at a potential 0.2~0.3V, lower than that of

Pt [69,70]. The sequence of catalytic activity of all the prepared catalysts toward formic acid oxidation is as following:

Pt-Ru(2:1)/PANI-POMAN(1:1)>Pt-Ru(1:1)/PANI-POMAN(1:1)>Pt-Ru(1:2)/PANI-POMAN(1:1)>Pt-Ru(1:0)/PANI-POMAN(1:1)>Pt-Ru(0:1)/PANI-POMAN(1:1).

Therefore, it can be concluded that certain amount of Ru metal can improve the catalytic activity of Pt-Ru catalyst. However as an auxiliary catalyst, Ru metal itself has no catalytic activity. Further increasing of Ru metal deposition can reduce the catalytic activity of the bimetallic catalyst [53].

4.4 Effect of scanning rate on catalytic oxidation to formic acid

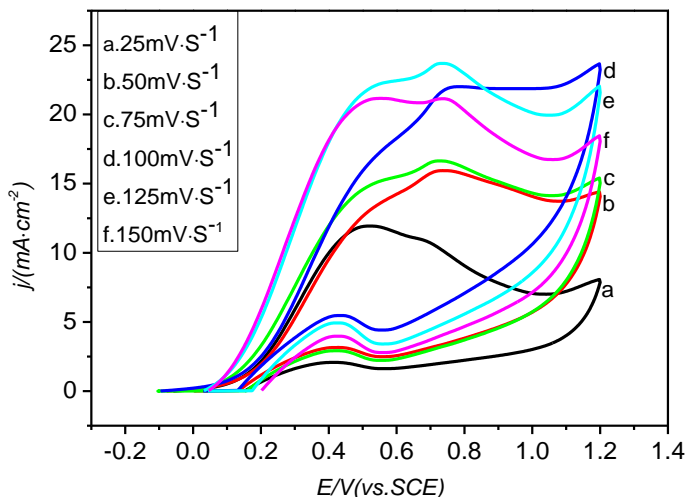


Figure 10. CV curves of Pt-Ru (2:1)/PANI-POMAN (1:1) composite catalyst in a $1\text{ mol}\cdot\text{dm}^{-3}\text{HCOOH} + 0.5\text{ mol}\cdot\text{dm}^{-3}\text{H}_2\text{SO}_4$ solution at different scanning rates

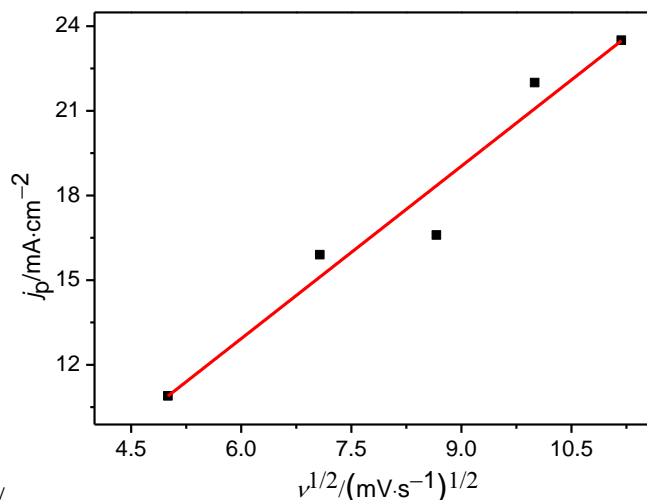


Figure 11. The relationship between the anode peak current density of formic acid oxidation at Pt-Ru(2:1)/PANI-POMAN(1:1) composite electrode vs. the square root of scan rates in a $1\text{ mol}\cdot\text{dm}^{-3}\text{HCOOH} + 0.5\text{ mol}\cdot\text{dm}^{-3}\text{H}_2\text{SO}_4$ solution

Fig.10 shows the CV curves of Pt-Ru (2:1)/PANI-POMAN (1:1) composite catalyst in the $0.5\text{ mol}\cdot\text{dm}^{-3}$ sulfuric acid solution containing $1\text{ mol}\cdot\text{dm}^{-3}$ formic acid at different scanning rates. The value

of the peak current density is mainly related to surface diffusion of the reactants on the electrode surface due to concentration gradient. Normally the concentration gradient decrease with time. The longer the oxidation time is, the smaller the peak current density become. As illustrated in Fig.10, the peak current density increases significantly with the scanning rate in the range of 25 to 125mV·s⁻¹. When the scan rate is increased and the scan time decreases, the increase of concentration gradient results in a large peak current density. However, when the scan rate is larger than 125mV·s⁻¹, the peak current density decreases possibly due to the depletion of the reactants within the short reaction time. Fig. 10 shows the effect of scan rate on the electro-oxidation of formic acid on the Pt-Ru (2:1)/PANI-POMAN (1:1) composite electrode. It can be observed from Fig.11 that the anodic peak current density is linearly proportional to the square root of scan rates, which suggests that the electrocatalytic oxidation of formic acid on Pt-Ru (2:1)/PANI-POMAN (1:1) composite electrode is a diffusion-controlled process. Indicating that the diffusion process will affect the catalytic oxidation of Pt-Ru bimetallic catalyst [44,71].

4.5 Stability of the catalysts

The catalyst stability can be characterized by measuring the current density as a function of time. Fig.12 shows the stability curves of Pt/PANI-POMAN (1:1) and Pt-Ru/PANI-POMAN (1:1) composite electrodes.

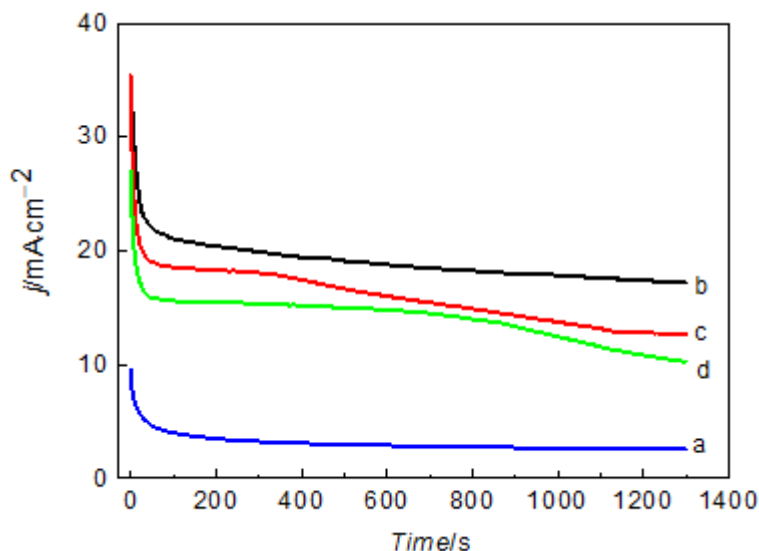


Figure 12. Timing current curves of different ratios of Pt to Ru on PANI-POMAN film in a 1mol·dm⁻³ HCOOH+ 0.5mol·dm⁻³ H₂SO₄ solution, The scanning potential is 0.75v, a. Pt/PANI-POMAN (1:1), b. Pt-Ru (2:1)/PANI-POMAN (1:1), c. Pt-Ru (1:1)/PANI-POMAN (1:1), d. Pt-Ru (1:2)/PANI-POMAN (1:1)

As illustrated, Ru modified Pt composite electrodes have significant improvement in catalytic activity and stability. In the whole current decay process (1300s), the current densities of three bimetallic catalysts are much higher than that of the pure Pt catalyst. Particularly Pt-Ru(2:1)/PANI-POMAN(1:1) catalyst not only has the maximum initial current density, but also can maintain the

highest current density $17\text{mA}\cdot\text{cm}^{-2}$ which is 5 times higher than that of Pt/PANI-POMAN(1:1) electrode. It indicates that Pt-Ru (2:1)/PANI-POMAN (1:1) catalyst has much better stability and poison resistance [72]. It may be due to Pt Ru metal particles embedded in the composite film of polyaniline-poly-(*o*-methoxyaniline), the polymer film can play a role in fixing the nanoparticles. The nanoparticles could not aggregate during the long scanning time. It illustrated that Pt-Ru (2:1)/PANI-POMAN (1:1) composite catalyst has good electrochemical activity. In addition, another current time curves under different potentials in fig.13 also showed that the catalyst also has good stability. The surface morphology SEM of Pt-Ru (2:1)/PANI-POMAN (1:1) catalyst after catalytic oxidation of $1\text{mol}\cdot\text{dm}^{-3}$ HCOOH+ $0.5\text{mol}\cdot\text{dm}^{-3}$ H₂SO₄ solution turn out that the metal nanoparticles were still remained in the surface of the polymer film.

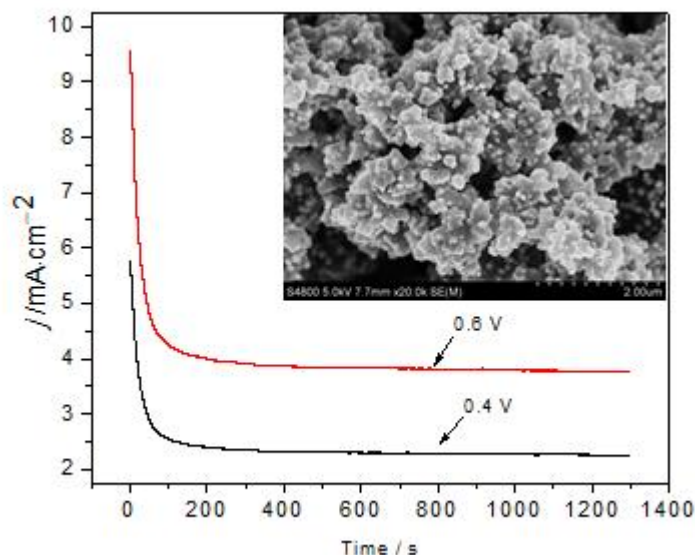


Figure 13. Timing current curves of catalytic oxidation of $1\text{mol}\cdot\text{dm}^{-3}$ HCOOH+ $0.5\text{mol}\cdot\text{dm}^{-3}$ H₂SO₄ solution by Pt-Ru (2:1)/PANI-POMAN (1:1) at different potential; the surface morphology SEM of Pt-Ru (2:1)/PANI-POMAN (1:1) catalyst after catalytic oxidation of $1\text{mol}\cdot\text{dm}^{-3}$ HCOOH+ $0.5\text{mol}\cdot\text{dm}^{-3}$ H₂SO₄ solution

5. CONCLUSION

In this paper, a durable and highly efficient Pt-Ru (2:1)/PANI-POMAN (1:1) composite electrode for DFAFCs has been successfully developed by CV method in aqueous acid solution using the three-electrode system. SEM results show that PANI-POMAN (1:1) substrate has a unique plate-like morphology with large surface area and porous layered structure to uniformly distribute and disperse Pt-Ru bimetallic particles. The introduction of Ru metal into Pt catalyst can significantly improve the catalytic activity and stability of Pt catalyst, promoting the direct oxidation of formic acid oxidation and greatly inhibiting the indirect oxidation. Therefore, Pt-Ru (2:1)/PANI-POMAN (1:1) composite is a promising candidate for future fuel cells devices.

ACKNOWLEDGMENTS

The research was supported by the Hunan Provincial Natural Science Foundation of China (13JJ5018), the Key Technology R&D Program of Hunan Provincial Science & Technology Department (2009FJ3138) and the Changsha Science & Technology Bureau (2012-64)

References

1. M.Weber, J.T.Wang, S.Wasmus and R.F.Savinell, *Journal of The Electrochemical Society*, 143(1996)158.
2. C.Rice, S.Ha, R.I.Masel, P.Waszczyk, A.Wieckowski and T.Barnard, *Journal of Power Sources*, 111(2002)83
3. S.Ha, C.A.Rice, R.I.Masel and A.Wieckowski, *Journal of Power Sources*, 112 (2002) 655
4. C.Rice, S.Ha., R.I.Masel and A. Wieckowski, *Journal of Power Sources* , 115(2003) 229
5. Y.W.Rhee, S.Y.Ha and R.I.Masel, *Journal of Power Sources* , 117(2003) 35
6. S.Ha, , B.Adams and R.I.Masel, *Journal of Power Sources* , 128(2004)119
7. Y.M.Zhu, S.Y.Ha and R.I.Masel, *Journal of Power Sources*, 130(2004) 8.
8. X.Wang, J.M.Hu , and I.M.Hsing, *Journal of Electroanalytical Chemistry* , 562(2004)73.
9. S.Ha, R.Larsen, Y.Zhu, and R.I.Masel, *Fuel Cells*, 4(2004)337
10. S.Ha, R.Larsen and R.I.Masel, *Journal of Power Sources* , 144(2005)28
11. Y.M.Zhu, Z.Khan and R.I.Masel, *Journal of Power Sources* ,139(2005)15
12. R.S.Jayashree, J.S.Spendelow, J.Yeom, C.Rastogi, M.A.Shannon and P.J.A.Kenis, *Electrochimica Acta*, 50(2005)4674
13. J.Yeom, G.Z.Mozsgai, B.R.Flachsbart, E.R.Choban, A.Asthana, M.A.Shannon and P.J.A.Kenis, *Sensors and Actuators B: Chemical*,107(2005)882
14. K.L.Chu , S.Gold, V.Subramanian, L.Chang,M.A.Shannon and R.I.Masel, *Microelectromechanical System* ,15(2006)671
15. Z.L.Liu, L.Hong, M.P.Tham, T.H.Lim and H.X.Jiang, *Journal of Power Sources* , 161 (2006)831
16. L.L.Zhang, T.H.Lu, J.C.Bao, Y.W.Tang and C.Li, *Electrochemistry Communications*, 8(2006) 1625
17. J.H.Choi, K.J.Jeong, Y.Dong, J.Han, T.H.Lim, J.S.Lee and Y.E.Sung, *Journal of Power Sources* ,163(2006)71
18. S.Ha, Z.Dunbar and R.I.Masel, *Journal of Power Sources* , 158(2006)129
19. J.Yeom, R.S.Jayashree,C.Rastogi, M.A.Shannon and P.J.A.Kenis, *Journal of Power Sources*, 160(2006)1058
20. C.M.Miesse, W.S.Jung, K.J.Jeong, J.K.Lee, J.Han, S.P.Yoon, S.W.Nam, T.H.Lim and S.A.Hong , *Journal of Power Sources*, 162(2006)532
21. K.J.Jeong, C.M. Miesse, J.H.Choi, J.Lee, J.Han, S.P.Yoon, S.W.Nam and T.G.Lee, *Journal of Power Sources*, 168(2007)119
22. F.L.Chen, M.H.Chang and M.K.Lin, *Electrochimica. Acta*, 52(2007)2506
23. X.C.Zhou, W.Xing, C.P.Liu and T.H.Lu, *Electrochemistry Communications*, 9(2007) 1469
24. S.Uhm, S.T. Chung and J. Lee, *Electrochemistry. Communications*, 9(2007)2027
25. A.Kundu, J.H.Jang, J.H.Gil, C.R.Jung, H.R.Lee, S.H.Kim, B.Ku and Y.S.Oh, *Journal of Power Sources* 170(2007)67
26. W.Chen, Y.W.Tang, J.C.Bao, Y.Gao, C.P.Liu, W.Xing and T.H.Lu, *Journal of Power Sources* 167(2007)315
27. X.W.Yu and P.G.Pickup, *Journal of Power Sources* , 182(2008)124
28. U.B.Demirci, *Environment International*,35(2009)626
29. A.Capon and R. Parsons, *Journal of Electroanalytical Chemistry and Interfacial*, 45(1973)205
30. N.Kristian, Y.L.Yu, P.Gunawan, R.Xu, W.Q.Dong, X.W.Liu and X.Wang, *Electrochimica . Acta*,

- 54(2009)4916
31. B.Liu, H.Y.Li, L.Die, X.H.Zhang, Z.Fan and J.H.Chen, *Journal of Power Sources*, 186 (2009)62
 32. J.S.Huang, H.Q. Hou and T.Y.You, *Electrochemistry Communications*, 11(2009)1281
 33. J.Lipkowski and P.N.Ross, *The Science of Electrocatalysis on Bimetallic Surface*, Wiley, New York, 1998, p63.
 34. K.M.Kost, D.E.Bartak, B.Kazee and T.Kuwana, *Analytical Chemistry*., 60(1988)2379
 35. H.Gharibi, M.Zhiani, R.A.Mirzaie, M.Kheirmand, A.A.Entezami, K.Kakaei and M.Javaheri , *Journal of Power Sources*, 155(2006)138
 36. E.K.W.Lai, P.D.Beattie, F.P.Orfino, E.Simon and S.Holdcroft, *Electrochimica. Acta*, 44 (1999) 2559
 37. Z.W.Chen, M.Waje, W.Z. Li and Y.S.Yan, *Angewandte Chemie International Edition*, 49(2007)1
 38. J.Han, G.P.Song and R.Guo, *Advanced Materials*., 19(2007)2993
 39. G.Wu, L. Li, J.H.Li and B.Q.Xu, *Carbon*, 43(2005)2579
 40. Y.T.Xu, X.L. Peng, H.T.Zeng, L.Z.Dai and H.H.Wu , *Comptes Rendus Chimie* ,11(2008)147
 41. D.Profeti and P.Olivi, *Electrochimica Acta*, 49(2004)4979
 42. F.Fıçıcıoğlu and F.Kadırgan, *Journal of Electroanalytical Chemistry*, 430(1997)179
 43. P.A.Christensen and A.Hamnett, *Techniques and Mechanisms in Electrochemistry*, Blackie Academic, London, 1994, Chapter 3: 3.4.2.1 Structure.
 44. W.Q.Zhou, C.Y.Zhai, Y.K.Du, J.K.Xu and P.Yang, *International Journal of Hydrogen Energy*, 34(2009)9316
 45. E.M.Guerra and H.P. Oliveira, *Journal of sol-gel science and technology*, 50(2009)103
 46. B.Habibi, M.H.Pournaghi-Azar, H.Abdolmohammad-Zadeh and H.Razmi, *International Journal of Hydrogen Energy* , 34(2009)2880
 47. A.L.Dyer and J.R.Reynolds, in *Handbook of Conducting Polymers*, 3rd ed. (Eds: T. Skotheim, J. R. Reynolds), CRC Press, Taylor & Francis Group, Boca Raton, FL, 2006.
 48. C.W.Kuo, L.M.Huang, T.C.Wen and A.Gopalan, *Journal of Power Sources*, 160 (2006) 65
 49. L.Niu, Q.H.Li, F.H.Weil, S.X.Xu, P.P.Liu and X.L.Cao, *Journal of Electroanalytical Chemistry* , 578(2005)331
 50. A.Pozio, M.D.Francesco, A.Cemmi and F.Cardellini, *Journal of Power Sources*, 105(2002)13
 51. M.Sogaard, M.Odgaard, and E.M.Skou, *Solid State Ionics*, 145(2001)31
 52. L.Duić, Z.Mandić and S.Kovač, *Electrochimica Acta*, 40(1995)1681
 53. E.A.Franceschini, G.A.Planes, F.J.Williams, G.J.A.A.Soler-Illia and H.R.Corti , *Journal of Power Sources*, 196(2011)1723
 54. V. Radmilovic, H.A.Gasteiger and P.N. Ross, *Journal of Catalysis* , 154(1995)98
 55. E.S.Steigerwalt, G.A.Deluga and C.M.Lukehart, *The Journal of Physical Chemistry B*, 106 (2002) 760
 56. J.L.Haan, K.M.Stafford and R.I.Masel, *The Journal of Physical Chemistry C*, 114(2010) 11665
 57. Y.Y.Tong, H.S.Kim, P.K.Badu,P.Waszczuk, A.Wieckowski and E.Oldfield, *Journal of the americal chemical society* , 124(2002)468
 58. M.C.Gupta, and S.S.Umare, *Macromolecules*, 25(1992)138
 59. M.M.Musiani, *Electrochim. Acta*, 35(1990)1665
 60. A .Tarola, D.Dini, E.Salatelli, F. Andreani and F.Decker, *Electrochimica Acta*, 24(1999)4189
 61. V.V. Malev and V. V. Kondratiev, *Russian Chemical Reviews*, 2(2006)147
 62. W.J.Albery, C.M.Elliott and A.R. Mount, *Journal of Electroanalytical Chemistry and interfacial electrochemistry* , 288(1990)15
 63. F.Ren, R.Zhou, F.Jiang,W.Zhou,Y.Du,J.Xu and C.Wang , *Fuel cells*, 12(2012)116
 64. T.Takeguchi , T.Yamanaka , K.Asakura ,E.N.Muhamad,K,Uosaki and W.Ueda, *Journal of the American Chemical Society*, 134 (2012)14508
 65. C.Liao, Z.D.Weil, S.G.Chen,L. Li,M.B.Ji,Y.Tan and M.J.Liao, *The Journal of Physical Chemistry*

- C , 113(2009)5705
66. Q.Ge, S.Desai, M.Neurock, and K.Kourtakis, *The Journal of Physical Chemistry B*, 105(2001)9533
67. M. Krausa, and W.Vielstich, *Journal of Electroanalytical Chemistry*,379(1994)307
68. X.C.Zhou, C.P.Liu, J.H.Liao , T.H.Lu and Wei Xing ,*Journal of Power Sources*, 179(2008)481
69. T.Yajima , H.Uchida and M.Watanabe , *The Journal of Physical Chemistry B*, 108(2004)2654
70. F.F.Ren, F.X.Jiang, Y.K.Du,P.Yang,C.Y.Wang and J.K.Xu, *International Journal of Electrochemical Science*,6(2011)5701
71. Y.C.Zhao, X.L.Yang, J.N.Tian, F.Y.Wang and L.Zhan, *International Journal of Hydrogen Energy* , 35 (2010) 3249
72. Q.Z.Dong, Y.N.Li, L.Y.Zhu, T.Ma and C.C.Guo, *International Journal of Electrochemical Science*, 8(2013)8191

© 2014 The Authors. Published by ESG (www.electrochemsci.org). This article is an open access article distributed under the terms and conditions of the Creative Commons Attribution license (<http://creativecommons.org/licenses/by/4.0/>).